

# EXTENDING THE DEPTH OF FIELD IN MICROSCOPY THROUGH CURVELET-BASED FREQUENCY-ADAPTIVE IMAGE FUSION

Linda Tessens\*, Alessandro Ledda, Aleksandra Pižurica<sup>†</sup> and Wilfried Philips

TELIN  
Ghent University  
Sint-Pietersnieuwstraat 41  
B-9000 Ghent, Belgium  
Email: ltessens@telin.ugent.be

## ABSTRACT

Limited depth of field is an important problem in microscopy imaging. 3D objects are often thicker than the depth of field of the microscope, which means that it is optically impossible to make one single sharp image of them. Instead, different images in which each time a different area of the object is in focus have to be fused together. In this work, we propose a curvelet-based image fusion method that is frequency-adaptive. Because of the high directional sensitivity of the curvelet transform (and consequentially, its extreme sparseness), the average performance gain of the new method over state-of-the-art methods is high.

**Index Terms**— image restoration, image analysis, microscopy, focusing, wavelet transforms

## 1. INTRODUCTION

All optical imaging systems have a limited depth of field. Parts of a 3D object that fall outside the region that is within the focusing range of the imaging system, appear blurred in the image. This problem is particularly prevalent in conventional light microscopy. There, the object under investigation is often thicker than the depth of field of the microscope. By moving the object along the optical axis of the microscope, all parts of the object can be consecutively moved into the in-focus region of the microscope. In this way, a stack of images is produced, each containing blurred and in-focus parts of the objects. It is desirable to transform this stack to one single image that contains all the in-focus parts of the image stack. This can be achieved through fusion of the images in the stack (also called *slices*).

Many image fusion algorithms exist. An overview can be found in [1]. In this work as well as in [2], it is shown that wavelet-based approaches generally perform better than other methods for extended depth of field processing of images. Forster *et al.* developed a very promising technique based on the complex wavelet transform rather than on the real wavelet transform [3]. Using complex wavelets allows to distinguish between the detail information of the images (represented by the phase of the complex wavelet coefficients) and the weighting of this detail information (encoded in the magnitude of the wavelet coefficients). In this work, the importance of the choice of the image transform was illustrated.

In recent years, many novel geometric image transforms have been developed, such as the ridgelet transform [4], the wedgelet

transform [5] and the contourlet transform [6], just to name a few. These new transforms capture the geometric information present in images, and in this sense overcome the limitations of classical wavelets. Among these, a mathematically elegant method entitled the curvelet transform has gained increasing popularity [7]. Curvelets are directional basis functions that are highly localized, both in space and frequency. We refer the reader to [7] for a comprehensive description of the curvelet transform.

We propose an image fusion technique that exploits the excellent ability of the curvelet transform to separate high and low frequency image content. Because of the high directional sensitivity of the curvelet transform, *all* high frequency information present in an image, regardless of its orientation, is contained in the highest frequency curvelet sub-bands. These sub-bands are processed with a maximum absolute value selection rule similar to the one used in wavelet-based image fusion methods. For the remaining low-frequency sub-band, we propose a novel selection method that is based on inter-sub-band consistency.

The remainder of this paper is organized as follows. In Section 2, some practical background information on the curvelet transform is presented. In Section 3, we explain our curvelet-based image fusion method. Results are summarized in Section 4. We end with some concluding remarks in Section 5.

## 2. THE CURVELET TRANSFORM

Conceptually, the curvelet transform is a multi-scale pyramid with many directions and positions at each length scale [7]. Although it is originally a continuous transform [8], it has several digital implementations. The two most recent ones are introduced in [7]. There, one implementation is based on unequally-spaced fast Fourier transforms (USFFT), while the other one is based on the wrapping of specially selected Fourier samples [7]. We will use the latter throughout this paper. However, the use of the USFFT-based digital curvelet transform would lead us to similar results and conclusions.

The curvelet transform decomposes the image in several frequency scales. At the coarsest scale, isotropic wavelets are used as basis functions. At finer scales, curvelets take over this role.

Fig. 1b shows the curvelet decomposition of the test image in Fig. 1a into 4 frequency scales with 8 orientations at the coarsest curvelet scale. The low-pass image is located at the center of the representation. The curvelet coefficients are arranged around it. For representation purposes, we display the *magnitudes* of the coefficients. Those with value zero are marked in white, whereas coefficients with large magnitudes are dark. From the prevalent white

\*L.T. is supported as a research assistant of FWO Flanders.

<sup>†</sup>A.P. is supported as a postdoctoral research fellow of FWO Flanders.

color of Fig. 1b, it is clear that the curvelet decomposition of this image is extremely sparse.

The curvelet coefficients are grouped according to orientation and scale. The concentric coronae represent the different scales, starting with the lowest scale (low frequencies) in the center. Sub-bands of the same scale are ordered within these coronae so that the orientation suggested by their position matches the spatial frequencies they represent. E.g., a horizontal line will produce high curvelet coefficients in the sub-bands that are located directly above and below the low-pass image.

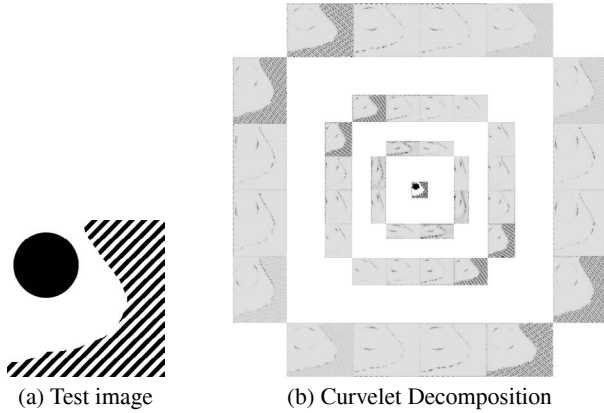


**Fig. 1.** (a) A  $256 \times 256$  test image. (b) Its curvelet decomposition into 4 scales and with 8 orientations at the coarsest scale. The low-pass image is located at the center of the representation. Curvelet coefficients with value zero are marked in white, whereas coefficients with a large magnitude are dark.

### 3. CURVELET-BASED IMAGE FUSION

To select the in-focus image parts throughout an image stack of a 3D object, we must be able to distinguish between in-focus and out-of-focus regions. Conceptually, edges and details appear to be ‘smeared out’ in blurred image regions. Mathematically, this means that a blurry image region contains less high frequencies than an in-focus one.

The sub-bands in the curvelet decomposition of an image can be considered as band-pass filtered versions of this image. Thus, high and low frequency image content are separated by this transform. The same is achieved by the wavelet transform, but only to a lesser extent. Indeed, as was mentioned before, the curvelet decomposition of a natural image is extremely sparse (a consequence of its high directional sensitivity). Every image feature is represented by a very limited number of non-zero curvelet coefficients. Virtually all information about high frequency image features is contained in the high frequency sub-bands of the decomposition. This means that blurring will primarily have an effect on the high frequency sub-bands, and the distinction between in-focus and out-of-focus image regions must thus be made here. Therefore, a curvelet decomposition into a small number of scales suffices to identify the in-focus image regions within the stack. In this work, we have used a decomposition into 3 scales (including the low-pass image). Image fusion based on a wavelet decomposition of the images into an equally small number of scales would lead to very poor results.

We will now discuss the different parts of our image fusion algorithm.

#### 3.1. Processing of the high frequency sub-bands

To process the high frequency sub-bands, we reason as follows. We know that big curvelet coefficients in the high-frequency sub-bands correspond to image features with a high spatial frequency (resolution). We assume these features lie in an in-focus image region. By selecting the coefficients throughout the stack with the highest absolute value at each position, orientation and scale, we assure that the most salient image features throughout the stack are preserved. This maximum absolute value selection rule is similar to the one used in many wavelet-based image fusion schemes (see [1, 2, 3]).

#### 3.2. Processing the low-pass image

By definition, the low-pass image contains only low frequency features. These features are not affected as strongly by blurring as high frequency image content. Therefore, the distinction between in-focus and out-of-focus image regions cannot be made at this scale, and the above-mentioned rationale to select the in-focus image parts throughout the stack by selecting the curvelet coefficients with the highest absolute value does not apply. Because we use only a very limited number of scales, a correct selection of the low-pass coefficients is very important, and therefore, we propose a novel strategy to perform this task.

This new strategy is based on the assumption of inter-sub-band consistency: all curvelet coefficients corresponding to a feature at a specific spatial location in the image should in theory be taken from the same slice, regardless of their scale and orientation. This means that the curvelet coefficients in the low-pass image should be taken from the same slice as the corresponding curvelet coefficients in the high-frequency sub-bands. As no such inter-sub-band consistency check was performed for the high-frequency sub-bands, not all corresponding curvelet coefficient will have been selected from the same slice. However, as an approximation, one can select the slice from which the majority of corresponding coefficients was selected. This assures that at each spatial position in the low-pass image, the curvelet coefficient from the correct, in-focus slice is selected.

#### 3.3. Image fusion algorithm

Our curvelet-based image fusion technique can be summarized as follows:

1. All images of the image stack are decomposed into their complex curvelet coefficients  $c_{i,j,z}(x,y)$ , where  $z$  denotes the slice index,  $i$  the scale and  $j$  the orientation within the scale.  $x$  and  $y$  are spatial coordinates.
2. For each point in every sub-band, the curvelet coefficient with the highest absolute value over all the slices in the stack is selected:

$$p_{i,j}(x,y) = c_{i,j,\text{argmax}_z(|c_{z,i,j}(x,y)|)}(x,y). \quad (1)$$

3. The low-pass image is processed (see Section 3.2).
4. The inverse curvelet transform of the curvelet coefficients  $p_{i,j}(x,y)$  is calculated.

#### 3.4. Pre- and Post-processing

As a pre-processing step, multi-channel images are first converted into gray-scale images by a weighted linear combination of the different channels:  $s_z(x,y) = \sum_k w_k s_z^{(k)}(x,y)$ . As was proposed

by Forster *et al.*, the weights  $w_k$  are obtained from a principal component analysis with the Karhunen-Loève transform (KLT). In this way, images with a predominant color will lead to gray-scale images with more contrast and saliency than if fixed weights were used [3].

After the inverse curvelet transform, the fused image may contain false gray-scale values. These are gray-scale values that were not present in any of the images of the image stack and thus may introduce artifacts. Forster *et al.* suggested to remove them through ‘reassignment’. Multi-channel reassignment for each channel  $k$  can be expressed as [3]:

$$q^k(x, y) = s_{\arg\min_z |p(x, y) - s(x, y; z)|}(x, y). \quad (2)$$

#### 4. RESULTS

To evaluate our curvelet-based image fusion method, we compare it with the complex wavelet-based method of Forster *et al.* [3], and with a pixel domain variance-based one. We test the methods both on artificially generated test data and on real microscopy images.

For all methods, the images are pre- and post-processed as described in Section 3.4.

To test the complex wavelet method, the artificial data is processed both with and without sub-band and majority consistency checks. The real microscopy images are processed without performing these checks, because, as Forster *et al.* pointed out in [3], these checks prove to be very costly with respect to storage space and computation time and are therefore best set aside for the processing of real microscopic stacks.

In the variance method, the distinction between in-focus and out-of-focus image regions is made based on the local variance. This local variance is calculated in a  $3 \times 3$  window around every pixel in every slice. At each spatial position in the fused image, the pixel from the slice with the highest local variance throughout the slice is selected.

##### 4.1. Artificial Test Data

To test our method in a quantitative way, we generated some artificial image stacks. The images used for this are displayed in Figure 2. The images *Eggs* and *Algae* are  $512 \times 512$  gray-scale microscopy images, the other images are  $512 \times 512$  color images of textures taken from the MIT Vision Texture Database. Each artificial stack is composed of three images. An example can be seen in Figure 3. In each of the three images, another part is left unblurred. The blurring is introduced through convolution with a  $5 \times 5$  Gaussian blurring kernel with standard deviation 1. Each stack is processed with the three fusion methods mentioned above. The result is compared with the original image. The resulting PSNR-values are grouped in Table 1.

From Table 1, we can see that for these stacks, the curvelet-based method outperforms the other methods. The average gain in PSNR over the variance method is 8.74 dB. Surprisingly, the complex wavelet method performs better without than with consistency checks, but also without checks, it lags behind the curvelet method by 3.02 dB on average. It is interesting to notice that the curvelet-based method performs particularly well for the *Eggs* image, which has many very sharp edges. On the contrary, the variance method produces a particularly poor result for this image. Indeed, the curvelet transform is particularly well suited for piecewise smooth images, whereas the variance method tends to introduce artifacts around abruptly-changing image structures. For the *Clouds* image, roles are reversed and the variance method even outperforms both multi-resolution methods.

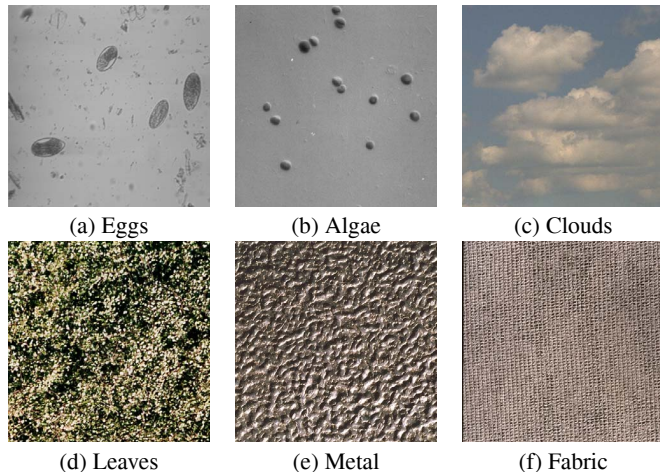


Fig. 2. The test images used for the creation of artificial test data.



Fig. 3. Example of an artificial image stack.

##### 4.2. Real Test Data

We now test the methods on a stack of 15  $512 \times 512$  color microscopic images of Peyer plaques from the intestine of a mouse<sup>1</sup>. The same images are used in [3]. Some slices are shown in Figure 4.

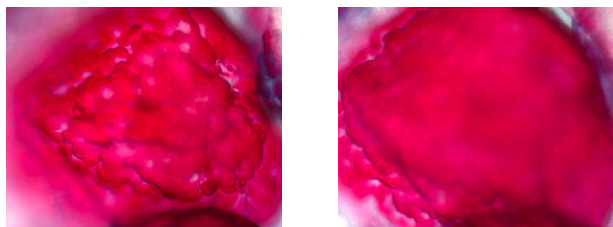


Fig. 4. Some slices of a stack of 15 microscopic images of Peyer plaques from the intestine of a mouse.

The image fusion results of the three tested methods are shown in Figure 5. As no ground-truth image is available, only a visual evaluation of the results is possible. We can see that in the image produced by the variance method, sharp edges are surrounded by artifacts. The complex wavelet-based method leaves some image regions blurred (see delineated regions). The curvelet-based method leads to a complete in-focus image, without introducing artifacts. This demonstrates that curvelets can be successfully used for image fusion of real microscopy image stacks.

<sup>1</sup>The images are courtesy of Jelena Mitic, Laboratoire d’Optique Biomédicale at EPF Lausanne, Zeiss and MIM at ISREC Lausanne.

**Table 1.** Image fusion results for different gray-scale and color image stacks, using the variance method, the complex wavelet-based method of Forster *et al.* [3] and the newly developed curvelet-based method.

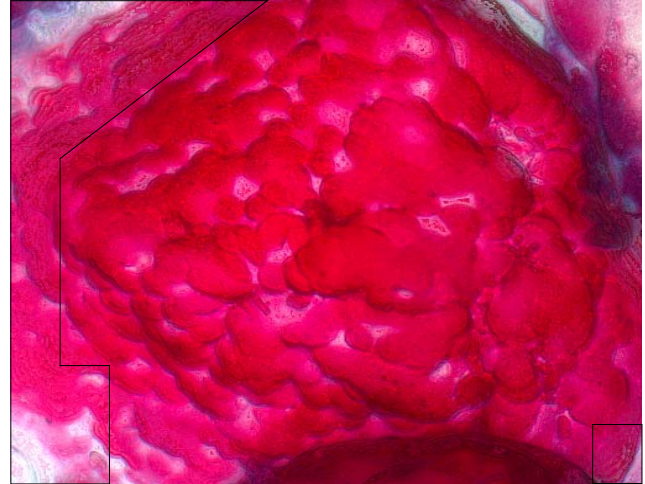
	Variance	Complex Db6	Complex Db6 with checks	Curvelets
Eggs	47.76dB	59.80dB	59.73dB	<b>65.82dB</b>
Algae	53.34dB	62.17dB	58.77dB	<b>63.92dB</b>
Clouds	<b>54.79dB</b>	49.26dB	49.21dB	52.73dB
Leaves	28.75dB	39.20dB	34.97dB	<b>41.27dB</b>
Metal	32.50dB	41.24dB	36.62dB	<b>44.18dB</b>
Fabric	41.47dB	41.25dB	35.50dB	<b>43.14dB</b>

## 5. CONCLUSION

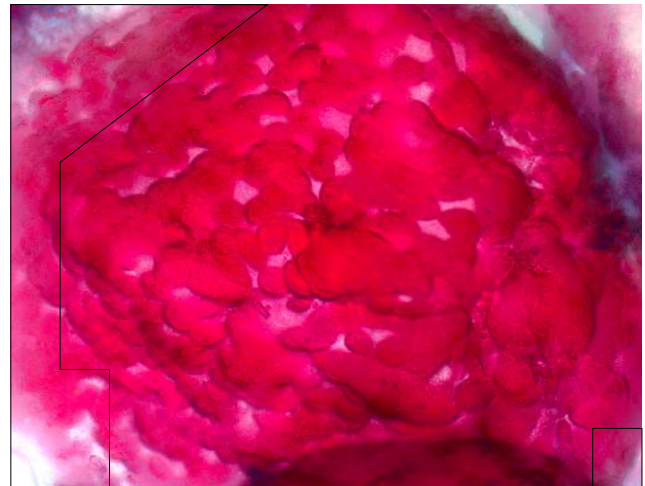
In this paper we have demonstrated that the directional sensitivity of the curvelet transform and its excellent ability to separate high and low frequency image content can be turned to good account to extend the depth of field of imaging systems. The proposed frequency-adaptive method produces high quality fusion results, both on real microscopy data and on artificially generated image stacks. Our method outperforms state-of-the-art fusion algorithms. The average performance gain is 3.02 dB over the complex wavelet-based technique of [3] and 8.74 dB over the discussed variance-based method.

## 6. REFERENCES

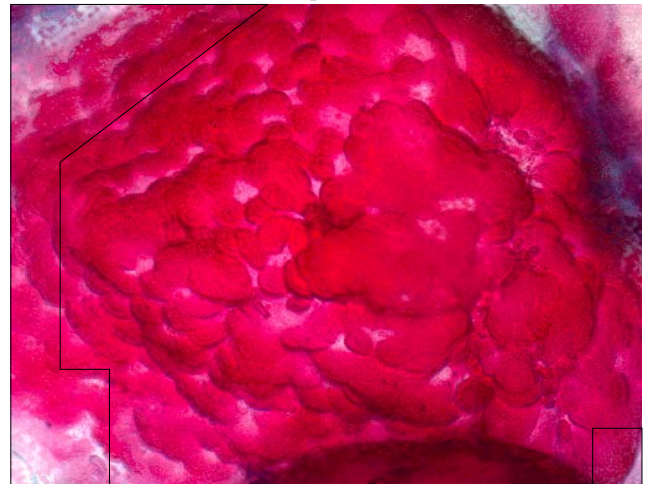
- [1] A.G. Valdecasas, D. Marshall, J.M. Becerra, and J.J. Terrero, "On the extended depth of focus algorithms for bright field microscopy," *Micron*, vol. 32, pp. 559 – 569, 2001.
- [2] H. Li, B.S. Manjunath, and S.K. Mitra, "Multisensor image fusion using the wavelet transform," *Graphical Models and Image Processing*, vol. 57, no. 3, pp. 235 – 245, 1995, Multisensor image fusion;.
- [3] B. Forster, D. Van De Ville, J. Berent, D. Sage, and M. Unser, "Complex wavelets for extended depth-of-field: A new method for the fusion of multichannel microscopy images," *Microscopy Research and Technique*, vol. 65, no. 1-2, pp. 33–42, September 2004, <http://bigwww.epfl.ch/publications/forster0404.html>.
- [4] E. J. Candes and D. L. Donoho, "Ridgelets: a key to higher-dimensional intermittency," *Phil. Trans. R. Soc. London A.*, pp. 2495–2509, 1999.
- [5] D.L. Donoho, "Wedgelets: nearly minimax estimation of edges," *The Annals of Statistics*, pp. 859–897, 1999.
- [6] Minh N. Do and Martin Vetterli, "The contourlet transform: An efficient directional multiresolution image representation," *IEEE Transactions on Image Processing*, vol. 14, no. 12, pp. 2091 – 2106, 2005.
- [7] E. J. Candes, L. Demanet, D. L. Donoho, and L. Ying, "Fast discrete curvelet transforms," Tech. Rep., Applied and Computational Mathematics, Caltech, 2005.
- [8] E. Candes, "The curvelet transform for image denoising," *IEEE International Conference on Image Processing*, vol. 1, 2001.



(a) Fusion result of the variance method.



(b) Fusion result of the complex wavelet-based method [3].



(c) Fusion result of the new curvelet-based method.

**Fig. 5.** Image fusion results of the three tested methods. In the image produced by the variance method, sharp edges are surrounded by artifacts. The complex wavelet-based method leaves some image regions blurred (see delineated regions). The curvelet-based method leads to a complete in-focus image, without introducing artifacts.